

# EXPERIMENTAL INVESTIGATION OF FLOW AROUND AEROFOILS WITH UNDULATING LEADING EDGES

**J. Pellicer**  
City University London, UK

*Keywords: undulations, tubercles.*

## Abstract

*An increase in aerodynamic performance at high angles of attack is observed in wings when their geometry is modified with the addition of biologically-inspired leading edge undulation. An experimental study was conducted at the Handley Page laboratory at City University London to investigate some details of the flow physics and shed some further light on the mechanisms by which the post-stall aerodynamic benefits are achieved. To this end, surface pressure and force balance measurements as well as flow visualization techniques were used on two wings of different aerofoil profile, before and after modifying their geometry with the inclusion of leading edge undulations. Pressure measurements and surface flow visualizations showed good agreement with results reported by previous work, replicating the increased suction peak in the line of minimum chord, more gradual stall onset and significant lift generated in the post-stall regime. Surface flow patterns reported by previous computational studies were also validated experimentally.*

## 1 Introduction

Leading edge undulations or tubercles, inspired by the morphology of the humpback whale fins has been the subject of a number of investigations in recent years, both experimentally and using computational methods. They act as passive flow control devices and for a certain range of Reynolds numbers, have been found to improve the aerodynamic performance of wings at high angles of attack, particularly in the post-stall

regime, without a significant drag penalty on the rest of the operation range.

Investigations on wings with undulating leading edges have been driven by the potential range of applications of these devices, since many types of lifting surfaces could benefit from a relatively simple passive flow controller, which would improve lift while reducing drag and noise when operating near and beyond their maximum lift coefficient. However, being a relatively new area of investigation, there is still opportunity for new research and validation of existing work.

The first rigorous study of the hydrodynamic capabilities of the humpback whale flipper was performed by Fish and Battle [1] who evaluated the morphology of a beached specimen's flipper to describe its shape in terms of hydrodynamically relevant parameters. They hypothesized the function of the tubercles to be analogous to vortex generators on aircraft wings, increasing the momentum transfer within the boundary layer and therefore maintaining the flow attached at higher angles of attack.

Miklosovic et al [2] created two idealized models of the whale flippers, with and without leading tubercles, based on a NACA0020 profile. A series of wind tunnel measurements were then performed between  $-2 < \alpha < 20^\circ$  and  $Re$  (based on the chord) of the order of  $5 \times 10^5$ . In general, they found the performance of the model with an undulating leading edge to be superior to that of the baseline model at most points of the operating range, especially at high angles of attack.

van Nierop et al [3] postulated that the mechanism responsible for the performance increase must be different from conventional vortex generators since the amplitude and wavelength of the tubercles is much greater than

the local boundary layer thickness. In support of their hypothesis, they performed an aerodynamic analysis based on thin airfoil theory with results reflecting general trends observed in previous experimental work [2] and showed an alteration to the pressure distribution on the wing based on the spanwise position.

A comprehensive investigation comparing the effect of variations on amplitude and wavelength of the tubercles on different airfoils was performed by Hansen, Kelso and Dally. [4] An optimal relation between amplitude and wavelength of the tubercles was proposed, being  $A/c = 3\%$  and  $\lambda/c = 11\%$ ; where  $c$  refers to the chord of the unmodified wing.

Skillen et al [5] performed a computational study using large-eddy simulation of a wing with an undulating leading-edge of amplitude and wavelength given by the optimal geometry in [4] and baseline NACA0021 profile in order to explain the mechanisms behind the performance gain. A strong suction peak and a separation bubble are evident in the regions of minimum chord and eventually the boundary layer is re-energized along the span of the wing, by means of secondary flow in the regions behind “peaks” and turbulent mixing in the regions behind “valleys”.

The aim of the present project was to study experimentally some of the characteristics of the flow around an unmodified (*baseline*) wing for direct comparison against those obtained with an undulating leading edge in order to provide experimental verification of the flow features identified by Skillen et al [5]. Pressure measurements and surface flow visualizations were carried out at an early stage in the project over a wing with a custom made airfoil section. It was then decided to extend the project with the addition of force balance measurements performed on a wing with a more conventional NACA0021 airfoil section, for the baseline and undulating LE cases, in order to study the response of the wing over a range of Reynolds numbers while keeping the geometry of the undulations constant.

## 2 Experimental methodology

The work was undertaken in the Handley Page Lab at City University London. Flow visualizations and pressure measurements were done in the T7 environmental wind tunnel while force measurements were taken using the overhead 6-axis balance available in the T2 wind tunnel. Both tunnels are closed loop with working sections of  $8 \times 3 \times 1.5\text{m}$  for T7 and  $1.12 \times 0.81 \times 1.78\text{m}$  for T2.

The wing used for pressure measurements and flow visualizations was manufactured in-house from wood with a maximum thickness of 17% located at 25% chord and a maximum camber of 1% located at 46% chord. Tip effects were controlled by the use of endplates.

The wing used for the force measurements was a standard NACA 0021 profile of 0.243m chord which was manufactured externally with a polystyrene foam core, a balsa veneer skin and a 20mm diameter silver steel rod running internally along the whole of the span, centred at  $0.25 x/c$  and protruding 200mm from one end to allow the model to be attached to the force balance. This wing was wrapped in thin black vinyl and a grid consisting of 256 fluorescent tufts with a 25mm spacing was created on one of the sides, covering whole span, to aid in determining the stall characteristics of the wing.

The tubercles used for the in-house wing in the early stages of the project were 3d printed individually, glued in position and faired into the wing using wood filler. This process was the most economic option considered and it prevented blockage of the pressure taps. However, it proved to be highly time consuming as many layers of wood filler were needed for a smooth finish while each layer took approximately a day to set.



Fig. 1. CAD models of NACA0021 baseline wing and tubercle sleeve.

For the force measurements a different arrangement was chosen where the baseline wing would serve as support for a “sleeve” of undulations which would be 3D printed in sections and simply slid into place to cover the whole span. The change in wing chord would then be compensated by adjusting tunnel speed to maintain the same Re as for the baseline wing.

Pressure distributions around the mid-span of the 17% thick wing were obtained by means of an array of miniature electronic pressure transducer interfaced to a CANdaq acquisition system connected to a PC with processing software provided by Aerotec, and compared with models generated using XFOIL code. Measurements were taken at incidences of 0, 5, 10, 15, 16, 17, 18, 19 and 20 degrees at a Re of  $2.5 \times 10^5$ .

After baseline flow visualizations had taken place, the wing was equipped with the set of tubercles and pressure measurements were taken following the same procedures as for the baseline wing. Due to misalignment between the suction and pressure tap lines of the model, only the suction side taps were used since taps in the pressure side were covered by the tubercle body.

The use of oil mixtures to obtain surface flow patterns has been a common technique for decades. The application of this technique in low speed wind tunnels was thoroughly studied

and reported in the AGARDograph 70 [6]. A number of tests were conducted on the baseline wing at 15m/s in order to determine the best mixture for the oil-flow visualizations. After small corrections to the formula proposed by Depardon et al [7], following suggestions given in [6], a satisfactory mixture based on white spirit, kaolin powder and oleic acid was obtained. Visualizations were performed on the baseline and modified wings at a Re of  $2.5 \times 10^5$  and incidences of 0, 5, 10, 15 and 20 degrees

A parametric force measurement study to investigate the efficiency of a given geometry of undulations to Re scaling was proposed for the NACA0021 wing. Measurements were taken at chord Re of 1.2, 2, 2.5, 3, and  $3.5 \times 10^5$ . The wing was then covered with the undulations and measurements repeated for the same Re values.

A 6-Axis overhead force balance with a computerized data acquisition system provided by Aerotech was also used to capture overall forces on the wing.

### 3 Results

#### 3.1 Pressure Measurements.

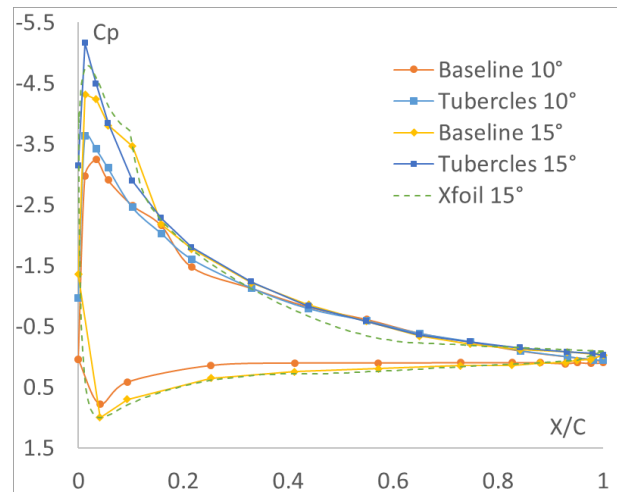


Fig. 2. Pressure measurements along the line of minimum chord for the 17% thick wing.

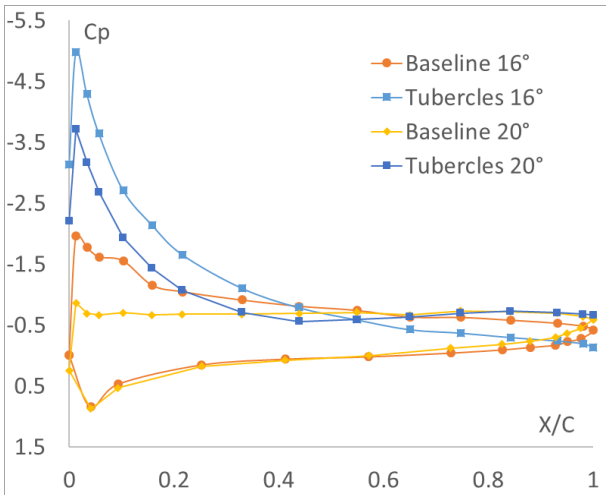


Fig. 3. Pressure measurements in the line of minimum chord for the 17% thick wing, stall and post stall.

Figures 2 and 3 above show the effect of the tubercles on the pressure distributions both pre- (Fig. 2) and post- (Fig. 3) stall. Fig. 2 includes a comparison with an XFOIL computation for the 15° case.

### 3.2 Flow Visualizations

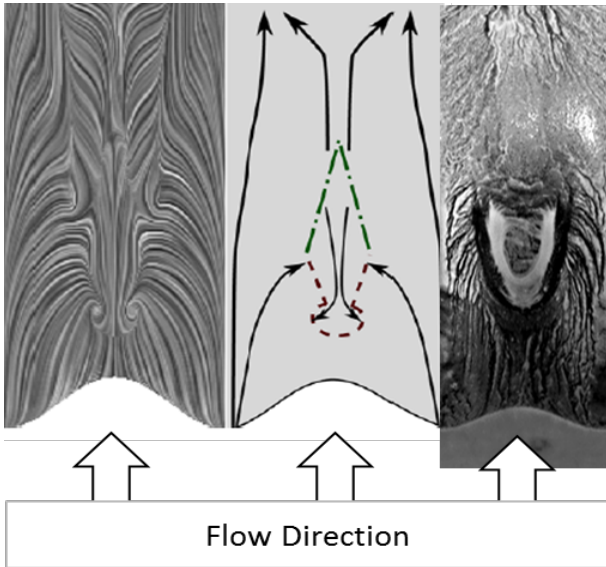


Fig. 4. Surface flow near the LE for the 20° case and comparison with experimental work [5]

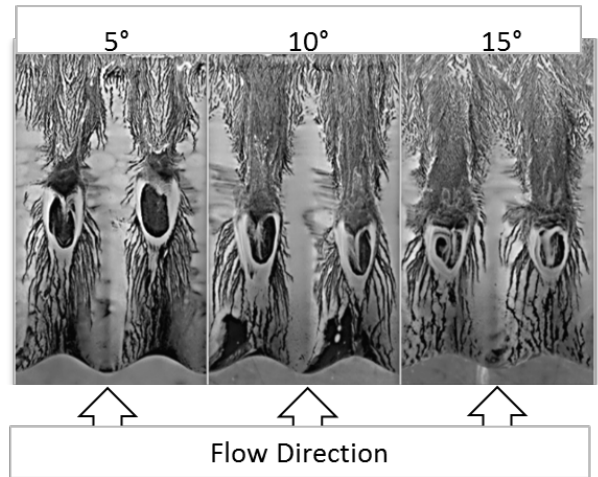


Fig. 5. Flow visualization around the LE for the 5, 10 and 15° incidence cases.

Figure 4 presents a comparison between the experimental oil flow visualization (right,  $Re\ 2.5 \times 10^5$ ), and the time-averaged wall shear stress (left,  $Re\ 1.2 \times 10^5$ ) and schematic of the surface flow topology (middle) produced by Skillen et al [5] in the vicinity of the LE for an incidence of 20°. Experimental surface oil flow visualizations for 5°, 10° and 15° incidence are shown in Fig. 5 ( $Re\ 2.5 \times 10^5$  for all cases).

### 3.3 Force Balance Measurements

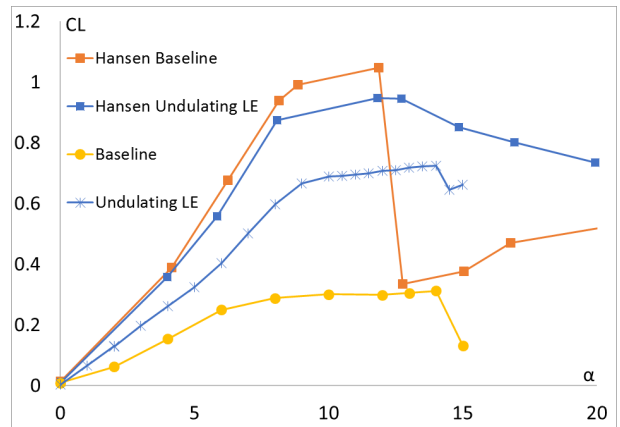


Fig. 6. Baseline and modified profile compared with previous experimental results [4].

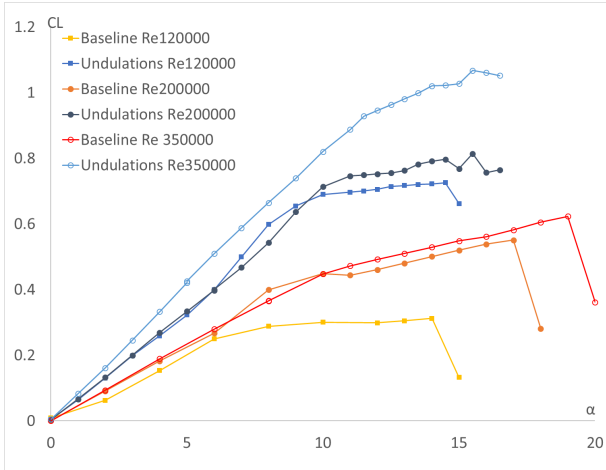


Fig. 7. Baseline and Undulating LE comparison for  $Re\ 1.2, 2$  and  $3.5 \times 10^5$

Figure 6 compares the lift polars obtained with the results reported by Hansen et al [4] for the NACA0021 wing ( $Re$  was  $1.2 \times 10^5$  in all cases). Owing to a mechanical problem the force balance had to be readjusted between the baseline and undulating LE cases, so these results are at best indicative pending further work. Figure 7 shows the lift polar sfor the NACA0021 baseline and modified wings at different Reynolds numbers. The polars corresponding to the undulated cases were obtained after the balance had been readjusted.

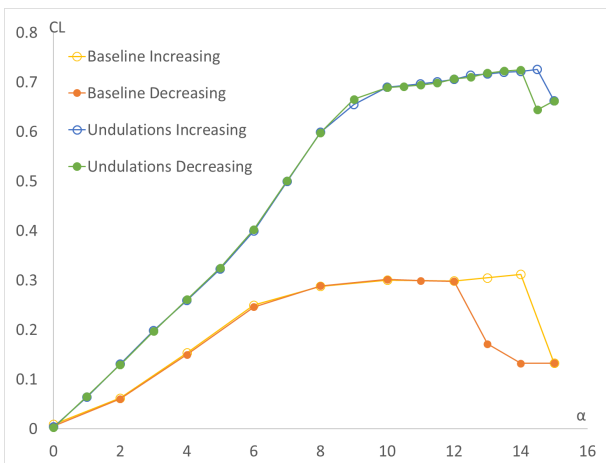


Fig. 8. Stall hysteresis,  $Re\ 1.2 \times 10^5$

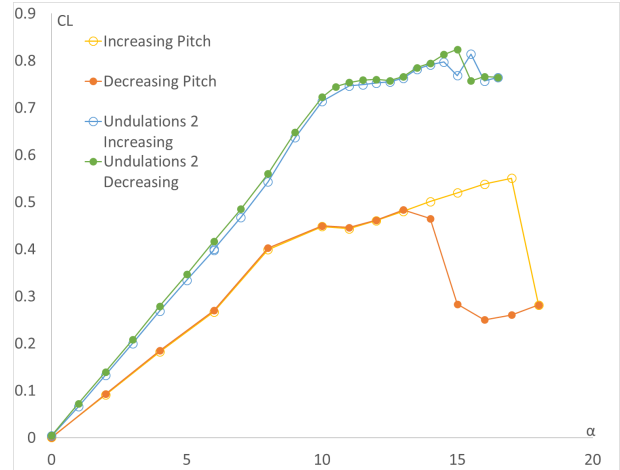


Fig. 9. Stall hysteresis,  $Re\ 2 \times 10^5$

Fig. 8 and 9 above show the stall behaviour of the baseline and modified wings at  $Re$  of  $1.2$  and  $2.5 \times 10^5$  respectively. Stall onset as the incidence increases is given by the blue and yellow lines for the modified and baseline wing. Once the wing has stalled, the incidence is then decreased until attachment is regained, shown by the green and orange lines for modified and baseline wing respectively.

## 4 Discussion

### 4.1 Pressure Measurements.

The chordwise pressure coefficient distribution for the clean wing case (Fig. 2) corresponds well with the results obtained from Xfoil. An increased suction peak is observed for both undulating cases when compared to the baseline wing at the same incidence: this behaviour has been reported in previous work [4] [5]. It can also be seen from this figure that the laminar separation bubble present in both baseline cases has disappeared when the wing is modified with undulations. This behaviour was previously reported by Hansen [8]

Figure 3 shows the pressure distribution for the  $16$  and  $20^\circ$  incidence cases. Here it can be seen that the baseline wing has stalled at  $16^\circ$ , but for the modified profile the presence of tubercles delays the onset of stall. Similar behaviour is seen for the  $20^\circ$  case, also in figure 3. Here the baseline wing is fully stalled and the modified wing, while indicating separation from  $40\%$  chord to the TE, still shows significant

suction up to 20% chord, indicating a more gradual stall.

#### 4.2 Flow Visualizations.

Good agreement is found between computational and experimental results in Fig. 4, even though the geometry of the aerofoil and  $Re$  differ for the experimental and computational analyses. The principal features of the flow are the same in each case, namely the presence of a separated region in the “valley” with flow from the “peaks” being drawn towards it. The dashed lines from the flow direction schematic represents a separation area, which is shown in the oil-flow picture as a black area enclosing a recirculating region.

The dash-dotted line in the flow schematic represents flow reattachment: this is better appreciated from in figure 5, which shows the experimental surface flow patterns at different incidences. Another interesting feature seen in this image is the location of the recirculation region which approaches the leading edge as the incidence increases, in much the same way as for a purely two-dimensional aerofoil flow.

#### 4.3 Force Balance Measurements.

Although the trends in lift coefficient are similar to those obtained by Hansen et al [4], there are discrepancies in the magnitudes of the values, particularly for the baseline case. These results led to a readjusting of the balance and in the following figures, all of the baseline measurements are shown pre-adjustment and all the undulating LE cases post-adjustment. However, this readjustment was made by hand and as the magnitude of the error present cannot be quantified at this point, none of the force balance measurements can be taken as conclusive.

Figure 7 shows slight improvements in  $C_{Lmax}$  as  $Re$  is increased. It is worth noting that for the undulating LE cases at higher  $Re$  ( $2$  and  $3.5 \times 10^5$ ) data was not acquired above  $16^\circ$  incidence in order to prevent overloading the balance.

Figures 8 and 9 show the hysteresis in the stall behaviour of the wing for the baseline and modified configurations, the undulating case after balance readjusting. For  $Re 1.2 \times 10^5$  the

baseline wing stalls when the incidence reaches  $14^\circ$ ; the incidence was then gradually lowered until the flow reattached at  $12^\circ$ . At this  $Re$  the modified wing stalls at the same incidence as the baseline wing, however flow reattaches as soon as the incidence is decreased to  $13^\circ$ . For  $Re 2 \times 10^5$  the baseline wing stalled at  $17^\circ$  and reattachment did not occur until the incidence was decreased to  $13^\circ$ . For this  $Re$  the undulated wing seems to stall at  $15^\circ$  and attachment is recovered at  $14.5^\circ$ ; this early stall, compared with the baseline case, was not expected. For all cases it can be seen that the stall onset is more gradual for the undulating LE cases, since  $dC_l/d\alpha$  is smaller than for the baseline cases. The flow also reattaches faster for the undulated cases when the incidence is decreased: this is in agreement with previous reports [3][4][8].

#### 5 Conclusion.

Pressure measurements and surface flow visualizations showed good agreement with results reported by previous work, replicating the increased suction peak in the line of minimum chord, more gradual stall onset and significant lift generated in the post-stall regime.

Experimental verification was also provided for the surface flow patterns in the vicinity of the leading edge undulations reported by [5]. Furthermore, these surface flow patterns were observed at all of the incidences studied.

Force measurements were less successful: only lift polars could be produced and for a smaller range of  $Re$  than initially planned, comparison with previous experimental data showed good agreement in terms of trends but not for force magnitudes. More gradual stall onset and recovery for the undulating LE compared with the baseline wing case was verified at different Reynolds numbers.

As a further recommendation, the use of LDA, could give an insight into the structure of flow field away from the surface, particularly in the regions of minimum chord and the “tubercle walls” surrounding them as the flow on these regions pose significant challenges to being studied by other methods due to the geometry of the tubercles.

## 6 References

- [1] Fish, F. E., & Battle, J. M. Hydrodynamic design of the humpback whale flipper. *Journal of Morphology*, Vol. 225, No.1, pp 51-60, 1995.
- [2] Miklosovic, D. S., Murray, M. M., Howle, L. E., & Fish, F. E. Leading-edge tubercles delay stall on humpback whale (*Megaptera novaeangliae*) flippers. *Physics of Fluids*, Vol. 16, No.5, pp L39-L42, 2004
- [3] van Nierop, E. A., Alben, S., & Brenner, M. P. How bumps on whale flippers delay stall: an aerodynamic model. *Physical review letters*, Vol. 100, No. 5, pp 054502. 2008.
- [4] Hansen, K. L., Kelso, R. M., & Dally, B. B. Performance variations of leading-edge tubercles for distinct airfoil profiles. *AIAA journal*, Vol. 49, No. 1, pp 185-194. 2011.
- [5] Skillen, A., Revell, A., Pinelli, A., Piomelli, U., & Favier, J. Flow over a Wing with Leading-Edge Undulations. *AIAA Journal*, Vol. 53, No. 2, pp 464-472. 2014.
- [6] Maltby, R. L. Flow visualization in wind tunnels using indicators. *AGARDograph*, Vol. 70, No. 1, pp 1-179, 1962.
- [7] Depardon, S., Lasserre, J. J., Boueilh, J. C., Brizzi, L. E., & Borée, J. Skin friction pattern analysis using near-wall PIV. *Experiments in Fluids*, Vol. 39, No. 5, pp 805-818. 2005.
- [8] Hansen, K. Effects of Leading Edge Tubercles on Airfoil Performance. *The University of Adelaide*. 2012

## Contact Author Email Address

jose.pellicer-collado.1@city.ac.uk

## Copyright Statement

The authors confirm that they, and/or their company or organization, hold copyright on all of the original material included in this paper. The authors also confirm that they have obtained permission, from the copyright holder of any third party material included in this paper, to publish it as part of their paper. The authors confirm that they give permission, or have obtained permission from the copyright holder of this paper, for the publication and distribution of this paper as part of the ICAS proceedings or as individual off-prints from the proceedings.